Memory effects in electrochemically gated metallic point contacts

R. Maul, F.-Q. Xie, Ch. Obermair, G. Schön, Th. Schimmel et al.

Citation: Appl. Phys. Lett. **100**, 203511 (2012); doi: 10.1063/1.4719207
View online: http://dx.doi.org/10.1063/1.4719207
View Table of Contents: http://apl.aip.org/resource/1/APPLAB/v100/i20
Published by the American Institute of Physics.

Memory effects in electrochemically gated metallic point contacts

R. Maul,[1,2,3] F.-Q. Xie,[1,4,5] Ch. Obermair,[1,4,5] G. Schön,[1,3,4] Th. Schimmel,[1,4,5,a)] and W. Wenzel[1,3,4,a)]
[1]*DFG-Center for Functional Nanostructures (CFN), Karlsruhe Institute of Technology, 76131 Karlsruhe, Germany*
[2]*Steinbuch Centre of Computing, Karlsruhe Institute of Technology, 76021 Karlsruhe, Germany*
[3]*Institut für Theoretische Festkörperphysik, Karlsruhe Institute of Technology, 76131 Karlsruhe, Germany*
[4]*Institute of Nanotechnology, Karlsruhe Institute of Technology, 76021 Karlsruhe, Germany*
[5]*Institute of Applied Physics, Karlsruhe Institute of Technology, 76131 Karlsruhe, Germany*

(Received 5 March 2012; accepted 28 April 2012; published online 18 May 2012)

Electrochemical gating permits the observation of few-atom processes in contact reconstruction. We monitor the junction conductance during the opening and closing of an atomic-scale metallic contact and use this as an instantaneous probe of the atomic-scale structural switching process. We observe clear correlations in the quantum conductance of a contact in subsequent switching events, demonstrating memory effects at the atomic scale. These experimental observations are supported by numerical simulations which show a conservation of the contact reconstruction process across several switching cycles. These results open a route to electrochemically control few-atom surface reconstruction events with present-day detection capabilities. © *2012 American Institute of Physics*. [http://dx.doi.org/10.1063/1.4719207]

The study of atomic-scale reconstruction processes within narrow, atomic-scale junctions and point contacts is a great challenge because there is no direct access for any scanning probe tip for geometrical reasons. Monitoring the motion of individual atoms and clusters of atoms during conformational changes of the surface is key for understanding the basic processes by which surface morphologies arise and change.[1] Investigation of such effects at or close to the tips of metal electrodes is also very important to understand electrode reconstruction in the course of single-molecule measurements in break junctions[2–6] or electromigrated metallic junctions,[7–10] in particular for metals that easily deform at the temperature of the experiment.[11] The role of metastable states in the formation of atomic-scale structures has been extensively studied in the context of metallic wires and molecular junctions using break-junction techniques and scanning tunneling microscopy (STM) analysis,[12,13] while simulations have elucidated the formation of magic clusters in metallic contacts, the creation of one-dimensional atomic chains, or the formation of molecular contacts. Here, we give insights by not only considering break-up but also reconstitution events that are accessible to date only in an electrochemical environment.

In recent work,[14–18] a single-atom transistor was demonstrated.[17] In this quantum electronic device, an electrical circuit is reproducibly opened and closed by the controlled and reversible movement of one single atom. The device, which can be operated at room temperature and at ambient conditions, is controlled by a voltage applied to an independent third electrode, the gate electrode. We demonstrated that reproducible bistable switching of silver quantum point contacts can be achieved by electrochemical control without any mechanical movement of an electrode—the only moveable part of the switch is the contacting atom. The preparation of the working electrodes and the electrochemical growth of silver atomic-scale point contacts have been described in detail in Ref. 17. The conductance signal is recorded at a low sampling rate of 20 samples/s and at a high sampling rate of 10^5 samples/s, respectively, with two computers. The slowly recorded signal is used for the switching control. The fast-recorded signal serves as a measure of the configuration of the contact. The experimental set-up is shown in Fig. 1(a). We could observe in experiment and simulation reversible bistable switching between open and conformations of the point contact with a variety of well-defined levels of quantum conductance.[15,17] This experimental setup provides an extraordinary amount of control over the process as the electrolyte acts as a natural buffer that translates any external signal into forces that are concentrated near the surface in the electrolyte double layer.[19] This makes it possible to generate a long sequence of controlled switching between the non-conducting and the quantized conducting state, as illustrated in Fig. 1(b) (slowly recorded signal), where the quantum conductance of the switch follows the gate potential.

The closing and opening of an atomic-scale contact are involving structural reorganization on the atomic scale. These structural changes of the contact area, in turn, have consequences on the conductance. Therefore, these atomic-scale structural reorganization processes in principle should be detectable in the conductance-vs.-time curves.

When we zoom in at the closing edges and the corresponding opening edges of switching events (displayed in Fig. 1(b) for three such events), we observe transient conductance changes (see Fig. 1(c)) in which the conductance varies stepwise on the whole but fluctuates in the process of closing the contact. The opening process finishes in one jump to open without intermediate plateaus between 0 and 1 G_0 ($G_0 = 2e^2/h$, e, electron charge, and h, Planck's constant, see Fig. 1(d)). The negative spikes come from the distribute capacitance in the measurement electronic circuits. In the open conformation, we observe small variations in the

a)Authors to whom correspondence should be addressed. Electronic mail: thomas.schimmel@kit.edu and wolfgang.wenzel@kit.edu.

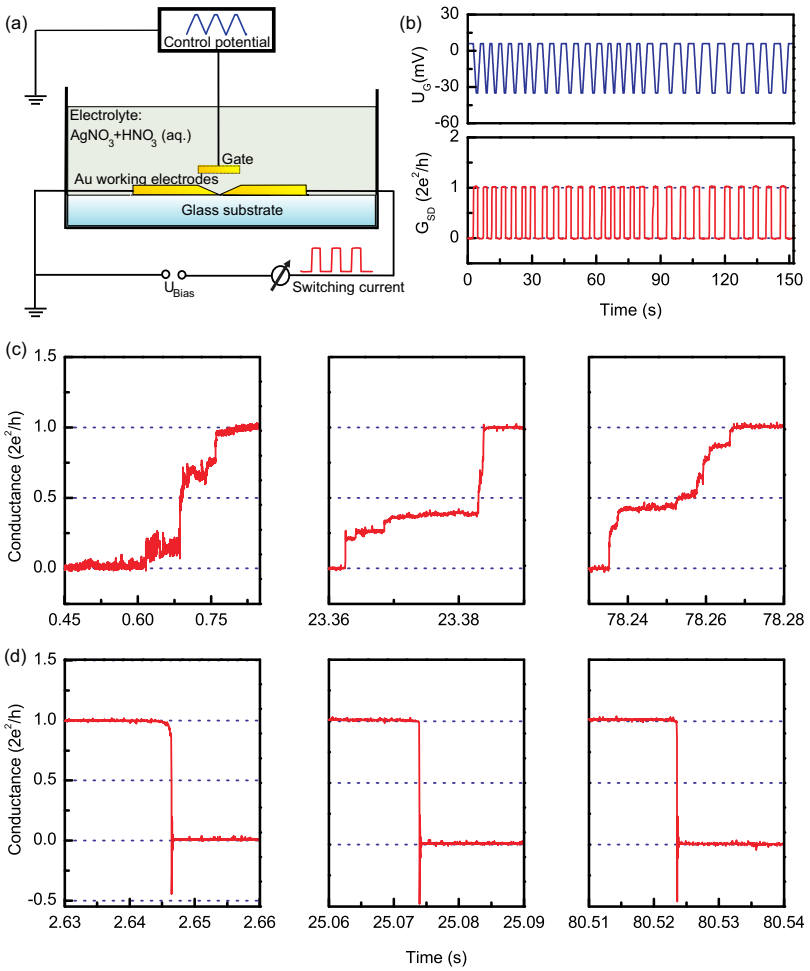

FIG. 1. Experimental observation of transient conductance changes at the closing and opening edges of switching events. The experimental set-up is shown in (a). A sequence of controlled switching events between the non-conducting "off-state" and the quantized conducting "on-state" is displayed in (b), where the quantum conductance of the switch follows the gate potential. The gate potential varies between 6 mV and −35 mV. Zoom-in at three experimentally observed closing events and the corresponding opening events contained in (b) is shown in (c) and (d) in 6 graphs, respectively. The negative spikes in (d) come from the measurement electronic circuits.

current that correspond to leakage effects through the electrolyte, which are followed by large changes in the current when the junction closes (or opens). Inspection of several data sets, such as those shown in Fig. 1(c), suggested that the observed plateaus in the conductance are not entirely random but may actually be a fingerprint of the reconstruction process.

In order to test this hypothesis, we have collected long trajectories of switching events for different junctions monitoring the conductance every 20 μs, similar to those gathered for the interpretation of current-voltage (I–V)-characteristics in break-junction single-molecule experiments.[20,21] In order to analyze the data, we have broken the trajectories into individual opening or closing events. Three such closing events are plotted in Fig. 1(c) as examples. For the statistical analysis we considered the conductance data taken during the closing events, discarded all data during the long periods where the junction was either fully open or fully closed (corresponding to zero and 1.0 G_0, respectively). Color coded histograms of the frequency of intermediate values of the conductance in subsequent switching cycles between 0.15 G_0 and 0.9 G_0 are displayed in Fig. 2(a) for 60 closing events. Every column of the plotted matrix represents one histogram with color-coded histogram-height. Intermediate conductance plateaus, visible as the bright spots in the figure, are observed repeatedly (though not in every switching cycle) as long as the contact remains stable. Overall, the fractional conductance values appear to follow a Poisson distribution, i.e., conductance values with low fractional conductance occur more often than those with high fractional conductance. The repeated occurrence of fractional conductance values in subsequent switching events indicated a correlation in the switching behavior. If switching proceeds by random dissolution and deposition processes of silver ions between the electrolyte and the electrode, one would expect different conformations, corresponding to different fractional conductance values, in subsequent switching events. However, inspection of the data suggests that subsequent switching events visit configurations with similar conductance, as indicated, for example, by the red circle marking switching events 18 to 28.

In order to quantitatively analyze correlation of subsequent switching events, we have computed the probability corrected pair-correlation function of all data,

$$f(c,c') = \int dt \rho(t,c)\rho(t+\delta t,c'), \tag{1}$$

which would result in a uniform distribution, if subsequent switching events are uncorrelated. Instead, the contour-plot in Fig. 2(b) shows a ridge along the diagonal, which indicates a significant correlation between subsequent intermediate levels in the conductance range below 0.5 G_0, corresponding to a memory effect in subsequent switching events. In order to quantify this memory effect, we have computed the time-correlation function between conductance values of subsequent switching events,

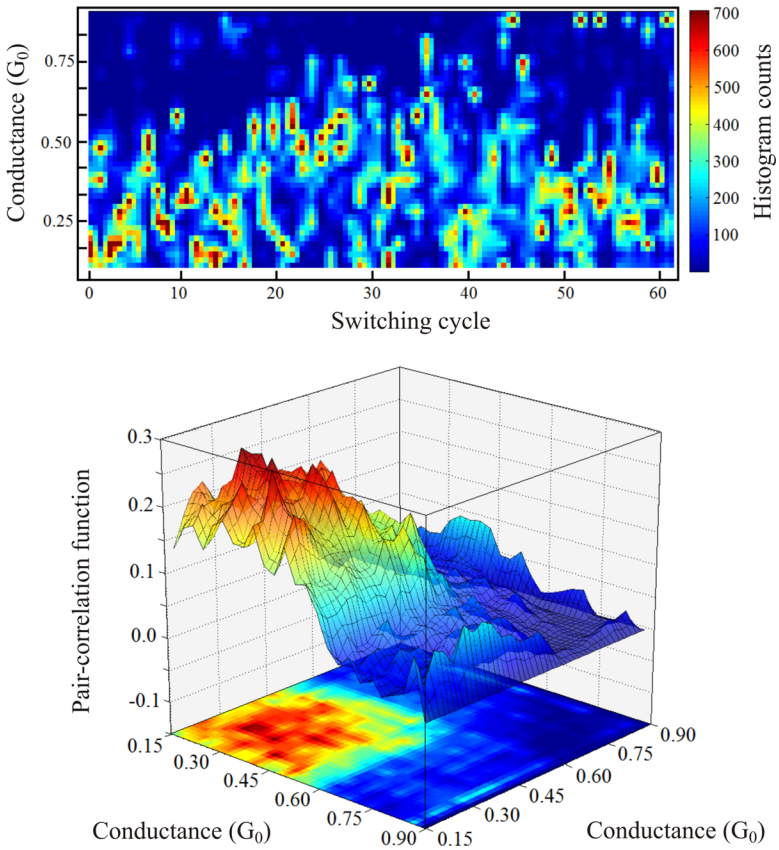

FIG. 2. (a) Color coded histograms of the frequency of intermediate values of the conductance in subsequent switching cycles between the "off" ($0\ G_0 = 2e^2/h$) state and "on" ($1\ G_0$). Every column of the plotted matrix represents one histogram with color coded histogram-height, the repeated occurrence of fractional conductance values in subsequent switching events indicated a correlation in the switching behavior. (b) Plot of the pair-correlation function f(c,c') for the sequence of conductance histograms. The contour-plot on the bottom of the graph shows a significant memory effect between subsequent intermediate levels in the range below $0.5\ G_0$. In the absence of correlation, the correlation function would be constant.

$$\zeta(\delta c) = \frac{1}{2\delta c}\int_{c-\delta c}^{c+\delta c}\int_{0}^{c'_{\max}}\int_{0}^{t_{end}} dc dc' dt \rho(t,c')\rho(t+\delta t,c). \quad (2)$$

As shown in Fig. 2(b), we observe a slow decay of correlation of subsequent switching events over many switching cycles ($0.25\ c^{-1}$).

To relate these observations to conformational changes in the reconstruction processes of the junction, we have performed all atom simulations, extending previous work in this direction.[14,15] We simulate the growth of silver point contacts[22,23] using a classical potential including surface charge effects and a model for the electrochemical double layer (EDL)[15,23] via the Gouy-Chapman model (GC).[24] This model treats the electrolyte with the linearized Poisson-Boltzmann's (PB) equation,

$$\nabla[-\varepsilon\nabla\phi(\vec{r})] = \sum_i z_i e c_i^{\infty} e^{\frac{z_i e\phi(\vec{r})}{kT}} \quad (3)$$

for the electrostatic potential $\phi(\vec{r})$. Here, ε denotes the permittivity of the solvent (water) $\varepsilon = \varepsilon_0\varepsilon_r$, z the charge of the ions (in units of the electron charge), and their bulk concentration c^{∞}. In our simulations, we solve this differential equation numerically in every step of the simulation and evaluate the electrostatic interactions on the basis of the potential induced by electrodes and the electrolyte. The thickness of the EDL is given by

$$\kappa^{-1} \approx \sqrt{\frac{2z^2e^2c^{\infty}}{\varepsilon kT}} = 10\text{Å} \quad (4)$$

in the model. In this layer of thickness, κ^{-1} being the distance from the left (L) or right (R) electrode, the electrode potential drops to φ_L/e or φ_R/e, respectively. Here, most screening effects and concentration changes (relative to the bulk) take place. The effect of considering the electrolyte is clearly visible when we analyze the distribution of the potential in a characteristic configuration of the silver quantum point contacts. In Fig. 3(a), we plot the color-coded potential $\phi(\vec{r})$ mapped to a sectional plane (of size $L \times H$, $L = 40$ Å, $H = 30$ Å) defined by $z = 0$. The potential varies between $\varphi_L < \phi(\vec{r}) < 0$, due to the presence of screening ions. In good agreement with the expected order of magnitude, we find $\kappa^{-1} = 10$ Å.

The assumptions made in the GC approach[24] (pointlike ions, PB distribution) may lead to an overestimation of κ^{-1} of the order of 30%, and depending on the bias voltage, model and experiment agree well within this framework ($\kappa^{-1} \sim 10$ Å). It is important to note, that even with possible errors in this range, the electrode-electrode distance in the moment when the junctions open or close is smaller than κ^{-1}. To make observation of plateaus in the conductance curve possible, we perform simulations with a very small displacement step size of 0.1 Å.

In each of these steps, we relax all atoms within a distance of 9.0 Å of the center of the junction using a simulated annealing protocol (5000 steps). This simulation relaxes the conformation to the adiabatic conformation corresponding to the given electrode-electrode distance. Reproducibly switchable junctions are observed in a significant fraction of growth simulations starting from silver electrodes placed far (5.6 nm) apart. These junctions form a contact that can be switched between two levels of quantum conductance by application of an electrochemical pressure induced by application of a small change in the gate potential. Once the

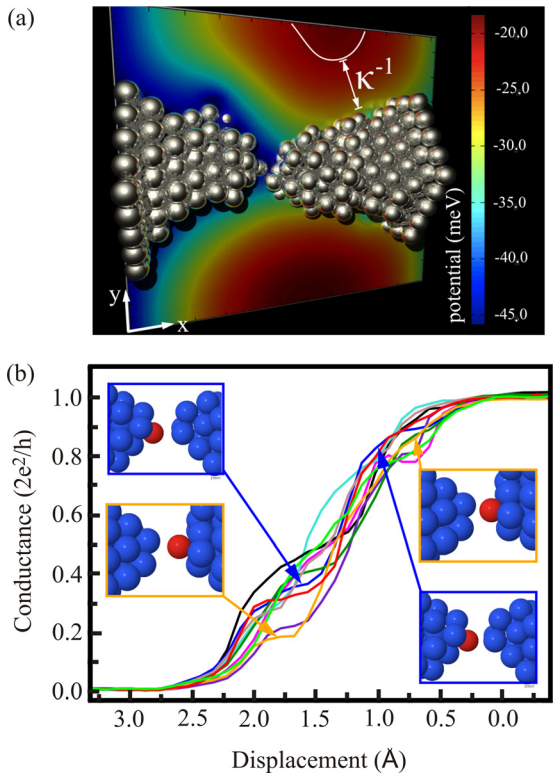

FIG. 3. (a) Electrostatic potential of single atom transistor screened by ions of the electrolyte. κ^{-1} denotes the thickness of the electrolytic double layer. (b) Total conductance of ten different single atom transistor conformations during a contact closing process in a computer simulation. All ten bi-stable conformations show weak plateaus at non-integer conductance values.

contact has formed, a training effect locks the two end-conformations corresponding to the open and closed conformation into reproducible geometries. This explains the stability of the switching process and excludes the occurrence of other conductance values at the endpoints of the switching process. In the following analysis, we focus on junctions with closed-junction conductance of 1 G_0, one example of which is shown in Fig. 3(a). Comparing simulations in vacuum[23] and with the electrolyte model, we notice that including the screening effect of the background charge modifies the contact growth process resulting in silver junctions with 15% larger diameter. This structural modification increases the stability of the switching mechanism.

We now look at multiple trajectories along the opening and closing processes in the simulation in detail. Analyzing the conductance as a function of electrode-distance (Fig. 3(b)), we observe plateaus at about 0.3 G_0 and 0.8 G_0 occurring typically at step electrode distances of 1.68 Å and 0.80 Å.

The occurrence of intermediate conductance values in the simulations suggests that the observed plateaus are the signature of the electrode reconstruction process as the junction closes. For the junctions investigated here, this corresponds to the motion of a single atom that recalibrates its position under the influence of the forces induced by the electrolyte and the electrodes. In order to switch between the open and the closed position, several atoms of the electrode must rearrange their position. Comparing experiment and simulation suggests that there are preferred pathways between these two conformations, which result in the observed memory effect.

The mechanism behind this phenomenon can be understood as follows: The potential energy surface has a barrier between the local energy minimum at the left and the right contact. When the junction is open or closed, the barrier between the two conformations is large, since both conformations are stable indefinitely in either conformation. When the silver contacts approach each other, the height of the barrier decreases. When it falls below the critical height $E_c = k_B T$, the thermal energy enables the silver atoms to hop from one energy minimum to the other and vice versa, leading to small conductance fluctuations until the minimum is unique at the closed state of the contact. While this process happens, there are one or more regions in electrode distance, where the energetic barrier inside the electrochemical double layer is low and the energy surface is rather flat. Within these regions, the junction geometry (and hence the conductance) changes little, resulting in a plateau in the conductance histogram.

To conclude, we were able to control the events at the atomic scale at the tip of the junction, which we can monitor via the conductance value. This was achieved by exploiting slow tuning of the conformation of a silver quantum point contact via an electrochemical control potential. We have observed distinct atomic-scale memory effects in subsequent switching events. These memory effects are only observed during the closing cycles of the atomic contacts. Clearly, no such effects are observed during the opening cycles. By making atomistic simulations, this could be explained by the existence of long-lived, metastable states of the junction during the closing process. These paths result in the observed highly correlated conductance values in subsequent switching cycles. Our experimental approach allowed the direct observation of single-atom processes in surface reconstruction. This also is of immediate relevance for understanding the breaking and formation of metallic point contacts that are now routinely used in single-molecule conductivity measurements.

The results allow a deeper understanding of atomic-scale reorganisation processes, which may help to better understand and ultimately control the complex physics at metallic surfaces. Thus, they open a route to electrochemically control the progress of fast surface reconstruction processes and make them observable within the detection capabilities of present-day experiments.

This work was supported by the Deutsche Forschungsgemeinschaft within the Center for Functional Nanostructures (CFN), Project Nos. B1.6, B5.1, and C3.6, and by the Baden-Württemberg Stiftung and the Ministry of Research and the Arts, Baden-Württemberg within the Network of Excellence "Functional Nanostructures."

[1]T.-L. Chan, C. Z. Wang, K. M. Ho, and J. R. Chelikowsky, Phys. Rev. Lett. **102**, 176101 (2009).
[2]C. A. Martin, D. Ding, J. K. Sørensen, T. Bjørnholm, J. M. van Ruitenbeek, and H. S. J. van der Zant, J. Am. Chem. Soc. **130**, 13198 (2008).
[3]W.-J. Hong, H. Valkenier, G. Mészáros, D. Zsolt Manrique, A. Mishchenko, A. Putz, P. Moreno Garcia, C. J. Lambert, J. C. Hummelen, and T. Wandlowski, Beilstein J. Nanotechnol. **2**, 699 (2011).
[4]E. Lörtscher, H. B. Weber, and H. Riel, Phys. Rev. Lett. **98**, 176807 (2007).
[5]T. Shiota, A. I. Mares, A. M. C. Valkering, T. H. Oosterkamp, and J. M. van Ruitenbeek, Phys. Rev. B **77**, 125411 (2008).

[6]M. L. Perrin, C. A. Martin, F. Prins, A. J. Shaikh, R. Eelkema, J. H. van Esch, J. M. van Ruitenbeek, H. S. J. van der Zant, and D. Dulić, Beilstein J. Nanotechnol. **2**, 714 (2011).
[7]S. Y. Quek, M. Kamenetska, M. L. Steigerwald, H. J. Choi, S. G. Louie, M. S. Hybertsen, J. B. Neaton, and L. Venkataraman, Nat. Nanotechnol. **4**, 230 (2009).
[8]M. Kamenetska, M. Koentopp, A. C. Whalley, Y. S. Park, M. L. Steigerwald, C. Nuckolls, M. S. Hybertsen, and L. Venkataraman, Phys. Rev. Lett. **102**, 126803 (2009).
[9]H. Song, Y. Kim, J. Ku, Y. H. Jang, H. Jeong, and T. Lee, Appl. Phys. Lett. **94**, 103110 (2009).
[10]M. Häfner, J. K. Viljas, and J. C. Cuevas, Phys. Rev. B **79**, 140410 (2009).
[11]J. Edwin Hobi, A. Fazzio, and A. J. R. da Silva, Phys. Rev. Lett. **100**, 056104 (2008).
[12]N. Agraït, A. L. Yeyati, and J. M. van Ruitenbeek, Phys. Rep. **377**, 81 (2003).
[13]C. Obermair, H. Kuhn, and T. Schimmel, Beilstein J. Nanotechnol. **2**, 740 (2011).
[14]F.-Q. Xie, R. Maul, S. Brendelberger, C. Obermair, E. B. Starikov, W. Wenzel, G. Schön, and T. Schimmel, Appl. Phys. Lett. **93**, 043103 (2008).
[15]F.-Q. Xie, R. Maul, A. Augenstein, C. Obermair, E. Starikov, G. Schön, T. Schimmel, and W. Wenzel, Nano Lett. **8**, 4493 (2008).
[16]F.-Q. Xie, R. Maul, C. Obermair, W. Wenzel, G. Schön, and T. Schimmel, Adv. Mater. **22**, 2033 (2010).
[17]F.-Q. Xie, L. Nittler, C. Obermair, and T. Schimmel, Phys. Rev. Lett. **93**, 128303 (2004).
[18]C. Obermair, F.-Q. Xie, and T. Schimmel, Europhys. News **41**(4), 25 (2010).
[19]J. Weissmüller, R. N. Viswanath, D. Kramer, P. Zimmer, R. Würschum, and H. Gleiter, Science **11**, 312 (2003).
[20]M. Kiguchi, O. Tal, S. Wohlthat, F. Pauly, M. Krieger, D. Djukic, J. C. Cuevas, and J. M. van Ruitenbeek, Phys. Rev. Lett. **101**, 046801 (2008).
[21]S. Y. Quek, L. Venkataraman, H. J. Choi, S. G. Louie, M. S. Hybertsen, and J. B. Neaton, Nano Lett. **7**, 3477 (2007).
[22]R. Maul and W. Wenzel, Phys. Rev. B **80**, 045424 (2009).
[23]D. M. Kolb, Angew. Chem. **40**, 1162 (2001).
[24]M. S. Kilic and M. Z. Bazant, Phys. Rev. E **75**, 021502 (2007).